

Toward a Practical X-Ray Fourier Holography at High Resolution

M. R. Howells¹, C. J. Jacobsen², S. Marchesini¹, S. Miller³, J. C. H. Spence^{1,3}, U. Weirastall³

¹Advanced Light Source, Lawrence Berkeley National Laboratory, Berkeley, CA 94720, USA.

²Department of Physics and Astronomy, SUNY, Stony Brook, NY 11794, USA.

³Department of Physics and Astronomy, Arizona State University, Tempe AZ 85287, USA

Introduction

We have described the advantages and history [1-4] of Fourier-transform x-ray holography as a potential high-resolution imaging scheme in an earlier paper [5]. In this paper we present some further arguments concerning the analysis of this type of diffraction problem and the derivation of high-resolution images from the measured data. We also report our experimental assessment of random pinhole arrays and aerogels as possible holographic reference objects.

Theory of Fourier-Transform Holography

Consider the plane-wave illumination of two objects producing exit-wave amplitudes f and g and angular spectra F and G respectively. We can show by standard Fourier-optics methods[6] that the intensity recorded by the detector (in the far field) is the Fourier transform hologram

$$I_H = |F|^2 + |G|^2 + FG^* \exp\left(\frac{2\pi i \mathbf{x}_1 \cdot \mathbf{b}}{l z}\right) + F^* G \exp\left(-\frac{2\pi i \mathbf{x}_1 \cdot \mathbf{b}}{l z}\right)$$

where the complex phase factors result from the spacing of the two objects, \mathbf{b} , according to the shift theorem. Normally we would regard one of the objects (say g) as the reference object and seek to make a reconstruction by illuminating the hologram by the original reference wave from g and back propagating the result to the object plane. We generalize that slightly here and use the wave from another object g' which may or may not equal g [7]. The resulting complex amplitude \mathbf{y} in the sample plane is then

$$\mathbf{y}(\mathbf{x}) = g' * R_{ff} + g' * R_{gg} + f(\mathbf{x} - \mathbf{b}) * R_{gg'} + f^*(-\mathbf{x} - \mathbf{b}) * (g' * g)$$

where $R_{gg'}$ is the cross correlation of g and g' . If we take g and g' to be delta functions or at least single sharp peaks then the usual four holographic image terms, the autocorrelation functions of f and g and the true and conjugate images, are visible in \mathbf{y} . Since this is an off-axis holographic scheme the twin images will be separated if the original objects are sufficiently separated.

Reconstruction of High Resolution Images: Deconvolution

We are interested in ways to achieve a high-resolution image without having to realize a point-like reference object. Therefore, following Stroke [7], we first note that the interesting true-image term is convolved with $R_{gg'}$. Thus if $R_{gg'}$ is sufficiently point-like, then a high-resolution image immediately results. One interesting case is when $g = g'$ and g is a random array of pinholes or other small objects. In this case $R_{gg'}$ reduces to the autocorrelation of a *single* object and a high-resolution true image again results. ($g * g'$ does not similarly reduce and the conjugate image does not reconstruct). There may be other ways in which $R_{gg'}$ can be made small, however we are also interested in the general case when g is known but $R_{gg'}$ is not small. In such a case a high-resolution image can still be recovered if a deconvolution can be implemented.

The standard way to do this starting from \mathbf{y} would be to calculate $F^{-1}\{F(\mathbf{y})/GG^*\}$. However we can do the same thing more directly by taking $F^{-1}\{I_H/G^*\}$. Evidently the power spectrum of g should be non-zero at all frequencies \mathbf{x}_1/lz for which we desire information. Unfortunately this is unlikely to

happen because, even for objects with the right spectral coverage like random pinhole arrays, the power spectrum (i. e. the diffraction pattern) will be a speckle pattern with many zeros. The way around this, which also allows some correction for spectral distortion due to noise, is to use a Wiener filter [8]. The recovered image is then

$$y_r(\mathbf{x}) = F^{-1} \left\{ I_H \frac{1}{G^*} \frac{|G|^2}{|G|^2 + F} \right\}$$

where F is the ratio of the noise power to signal power. This provides a pathway to high resolution for reference objects which are known. In principle this can also include unknown reference objects because one can holograph a pair of complex objects, a reference and a sample, placed with sufficient separation, and recover the structure of both via the iterative Fourier-transform algorithm [9]. A diffraction tomography experiment could then proceed by rotating the sample through at least 180° while keeping the reference object fixed in the position in which its exit-face wave function was measured.

Experiments and Results: Practical Reference Objects

We have made experimental tests of pinhole arrays and silica aerogels as candidate reference objects on beamline 9.0.1. The pinholes were about 10 nm in diameter and were produced by etching damage tracks made in 5- μm -thick mica plates by a 4 MeV α -particle beam. The aerogels were of pure silica, 3-4% dense and with peak pore size of 10-20 nm. We know, based on published hard x-ray small-angle patterns [10], that such materials have about the right spatial-frequency coverage, 0.1-0.001 \AA^{-1} , for high-resolution x-ray imaging. Ours were provided by Dr A. Hunt of the Lawrence Berkeley National Laboratory Division of Environmental Energy Technology. The choice of pinholes was based on the theoretical arguments advanced in the previous section plus the promise of easy measurement by standard scanned-probe or electron-microscope methods.

The candidate reference objects were illuminated by unmonochromatised undulator radiation ("pink beam") on beam line 9.0.1 at the Advanced Light Source at the Lawrence Berkeley National Laboratory. The beam was restricted by filters, apertures and a beam stop just in front of the CCD detector so that in the absence of diffraction by the sample, the count rate recorded by the detector was essentially zero. The beam consisted essentially of 100% 560 eV x-rays (for maximum absorption by mica) in the third undulator harmonic with coherence length of 120 waves and nominally perfect spatial coherence.

We were not able to observe the expected diffraction pattern and wave-guide effects from the pinhole arrays. This may have been due to blockage of the holes by contamination, although we did apply a standard countermeasure to that (a 10^{-4} torr background pressure of oxygen). Our observation of the holes by electron microscopy was necessarily done on a thin surface flake of mica which also leaves open the possibility of only partial penetration by the etchant. Reciprocity arguments suggest that alignment of the holes is not critical for pinholes of this size (diameter = $5I$).

On the other hand the aerogels gave good soft-x-ray scattering patterns with a spatial frequency cutoff corresponding to about 20 \AA resolution (Fig. 1).

Discussion and Conclusion

Although it is reassuring that aerogel reference objects seem to work well, we have to take into account that the scattering strength per unit volume is much reduced due to the low density. The requirement is that the integrated scattering strength of the reference should be at least as high as that of

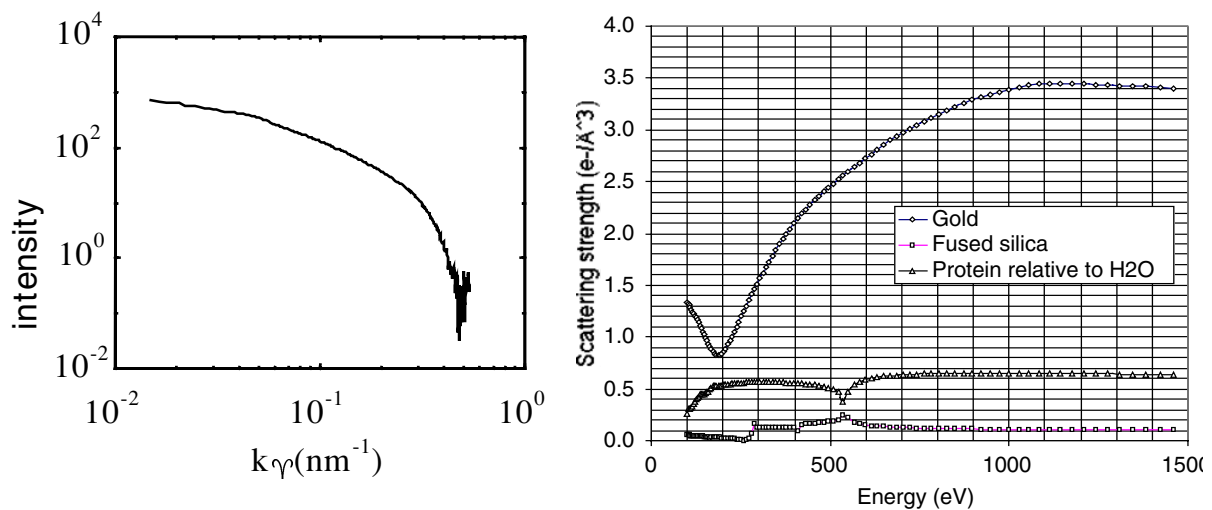


Fig. 1. (Left) Measured soft x-ray scattering pattern from a silica aerogel. (Right) Scattering strength of three interesting materials for designing a Fourier-holography experiment. Curves are calculated from tabulated atomic-scattering-factor data.

the biological sample material relative to its background of water. To help understand this issue we show in Fig. 1 the scattering strength of three important materials expressed in electrons per \AA^3 . The weaker scattering of the aerogels compared to the plotted values for normal silica, could be compensated in part by loading the aerogel with high Z material during manufacture and by simply making the reference object larger. Although estimates of the attainable scattering strength seem to rule out 2D arrays of gold spheres another interesting approach would be to construct a 3D array of such spheres by means of a variant of the normal labeling process.

Overall we believe that it is practical to build suitable reference objects for x-ray Fourier holography. Once this is done we also see a pathway to making a high-resolution deconvolution of the image at each view direction of the tilt series in spite of the inevitable zeros in the reference object diffraction pattern.

Acknowledgments

We wish to thank Arlon Hunt for supplying the aerogel samples, Tom Baer and Steven Kevan for helping us to get beam time and the US Department of Energy Office of Environmental and Biological Research for support under contract DE-FG02-89ER60858.

References

1. G. W. Stroke, *Appl. Phys. Lett.* **6**, 201 (1965).
2. J. T. Winthrop, C. R. Worthington, *Phys. Lett.* **15**, 124 (1965).
3. S. Aoki, Y. Ichahara, S. Kikuta, *Jpn. J. Appl. Phys.* **11**, 1857 (1972).
4. I. McNulty, J. Kirz, C. Jacobsen, E. Anderson, M. R. Howells, *Science* **256**, 1009 (1992).
5. M. R. Howells, B. Calef, C. J. Jacobsen, J. H. Spence, W. Yun, in *X-ray Microscopy*, W. Meyer-Ilse, A. Warwick, D. T. Attwood, Eds. (American Institute of Physics, Berkeley, 1999).
6. R. J. Collier, C. B. Burckhardt, L. H. Lin, *Optical Holography*. (Academic Press, New York, 1971).
7. G. W. Stroke, in *Optique des Rayons X et Microanalyse*, R. Castaing, P. Deschamps, J. Philibert, Eds. (Hermann, Paris, 1966).
8. K. R. Castleman, *Digital Image Processing*. (Prentice-Hall, Englewood Heights, 1979).
9. J. R. Fienup, *J. Opt. Soc. Am. A* **4**, 118 (1987).
10. D. W. Schafer, K. D. Keefer, *Phys. Rev. Lett.* **56**, 2199 (1986).

Principal investigator: Malcolm R. Howells, Advanced Light Source, Lawrence Berkeley National Laboratory.
Email: MR.Howells@lbl.gov. Telephone: 510-486-4949.